

Proton Transfers in the Nitrogen-Boron System at 27.5 Mev

E. NEWMAN

Oak Ridge National Laboratory, Oak Ridge, Tennessee*

(Received September 5, 1961)

The proton transfer reactions, (1) $B^{10}(N^{14}, O^{15})Be^9$, (2) $B^{10}(N^{14}, C^{13})C^{11}$, and (3) $B^{11}(N^{14}, C^{13})C^{12}$, leaving the reaction products in their ground states were investigated at a mean energy of the incident nitrogen ions of 27.5 Mev. To distinguish these reactions from other events, the two product particles were detected in coincidence by silicon surface-barrier counters. In addition, a proportional counter imposed the requirement that the observed particle have the correct charge. Angular distributions (1) and (2) peak at $r_0 \approx 2.2$ fermis when plotted as $d\sigma/dR_{\min}$ vs r_0 , where R_{\min} is the distance of closest approach for a Rutherford orbit and $r_0 = R_{\min}/(A_1^{1/3} + A_2^{1/3})$. The total ground-state cross sections were determined to be (1) 1.34 ± 0.30 mb, (2) 2.19 ± 0.49 mb, and (3) less than 0.3 mb. The data are compared with the predictions of the tunneling theory, and good agreement is found for the initial rise of the angular distribution.

I. INTRODUCTION

THE term transfer in conjunction with heavy-ion reactions is used to single out processes in which one or more nucleons make a transition from one nucleus to another. The field of nucleon transfers may be subdivided into three broad categories: (1) single-nucleon, proton, or neutron transfers; (2) multiple transfers, where two or more particles are transferred from one nucleus to the other; and (3) exchange transfers, in which at least two different nucleons are simultaneously exchanged between the interacting nuclei.

There has been considerable activity, both experimental and theoretical, in the field of single-nucleon transfer reactions. The reaction was first investigated by Reynolds, Scott, and Zucker¹ and by Chackett and Fremlin² at about the same time. As a result of a systematic study of single-neutron transfer reaction excitation functions,³⁻⁶ it was noted that essentially a "universal curve" exists when the total cross section is plotted as a function of E^* . The quantity E^* is defined as

$$E^* = E_{c.m.} - E_{barr} + Q$$

and is the kinetic energy available immediately after the transfer has taken place at the turning point of the incident orbit.

The angular distribution of reactions in which a neutron is transferred from the incident N^{14} ion to the target nucleus has been investigated at both low⁷⁻⁹ and

high energies.¹⁰⁻¹² These angular distributions have been measured by taking advantage of the radioactivity of the N^{13} end product. The scattered ions are caught on strips of aluminum placed so as to intercept a small range of scattering angles. These catchers are then counted to determine the amount of N^{13} present as a function of angle. Angular distributions of single neutron transfer reactions for projectiles other than N^{14} at high energies have also been studied by Kaufmann and Wolfgang¹³ using this method. For all of these experiments a peak in the angular distribution was found. If it is assumed that the incident and product particles travel on the same Rutherford orbit, then the position of the maximum in the angular distribution may be related to a classical distance of closest approach R_{\min}

$$R_{\min} = \frac{Z_1 Z_2 e^2}{2E_{c.m.}} [1 + \csc(\Theta/2)],$$

where Θ is the center-of-mass deflection angle. The parameter r_0 may then be evaluated from the relation

$$R_{\min} = r_0 (A_1^{1/3} + A_2^{1/3}).$$

Values for r_0 from the experiments above range from 1.45 to 1.67 fermis.

To determine the extent to which excited states contribute to transfer reactions several workers^{8,9,11} made simultaneous measurements of the angular distribution and, with stacked catcher foils, the range of the N^{13} particles. Essentially all the N^{13} detected were formed in their ground state, since excited states are unstable with respect to charged particle decay. It was found that an appreciable fraction of the transfers leave the other participating nucleus in excited states. Usually individual states are not distinguished so that most of

* Operated for the U. S. Atomic Energy Commission by Union Carbide Corporation.

¹ H. L. Reynolds, D. W. Scott, and A. Zucker, *Proc. Nat. Acad. Sci. U.S.A.* **39**, 975 (1953).

² K. F. Chackett and J. H. Fremlin, *Phil. Mag.* **45**, 735 (1954).

³ H. L. Reynolds and A. Zucker, *Phys. Rev.* **101**, 166 (1956).

⁴ H. L. Reynolds, D. W. Scott, and A. Zucker, *Phys. Rev.* **102**, 237 (1956).

⁵ M. L. Halbert, T. H. Handley, J. J. Pinajian, W. H. Webb, and A. Zucker, *Phys. Rev.* **106**, 251 (1957).

⁶ D. E. Fisher, A. Zucker, and A. Gropp, *Phys. Rev.* **113**, 542 (1959).

⁷ H. L. Reynolds and A. Zucker, *Phys. Rev.* **101**, 166, (1956).

⁸ M. L. Halbert and A. Zucker, *Phys. Rev.* **108**, 336 (1957).

⁹ K. S. Toth, *Phys. Rev.* **121**, 1190 (1961); *Phys. Rev.* **123**, 582 (1961).

¹⁰ V. V. Volkov, A. S. Pasiuk, and G. N. Flerov, *J. Exptl. Theoret. Phys. (U.S.S.R.)* **33**, 595 (1957) [translation: *Soviet Phys.—JETP* **6**, 459 (1958)].

¹¹ J. A. McIntyre, T. L. Watts, and F. C. Jobs, *Phys. Rev.* **119**, 1331 (1960).

¹² E. L. Hubbard and G. Merkel, *Proceedings of the Second Conference on Reactions Between Complex Nuclei, Gatlinburg* (John Wiley & Sons, New York, 1960), pp. 25-29.

¹³ R. Kaufmann and R. Wolfgang, *Phys. Rev.* **121**, 206 (1961).

these angular distributions, as well as others mentioned previously, sum contributions from many final states. Recently, however, Toth⁹ has measured the angular distribution of N^{13} from $N^{14}+N^{14}$ leaving the residual nuclei in specific states. In addition, he measured the relative yields for these states as a function of energy. It was found that only the ground and the first and/or the second excited state of N^{15} contribute to the transfer cross section in the 19.8–28 Mev energy range. In addition, it was noted that $r_0=2.2$ fermis is obtained from the ground-state transfer distributions while the excited state distributions result in an r_0 of approximately 1.65 fermis. The latter result may indicate that ground-state transfers occur at appreciably larger internuclear separation than transfers leaving the resulting products in excited states. However, the assumption that the outgoing particle follows the same Rutherford orbit as the projectile is especially doubtful for highly excited final states.

The theoretical aspects of nucleon transfer were first investigated by Breit and Ebel.¹⁴ They calculated the quantum-mechanical tunneling cross section for nuclei which do not overlap as they pass each other on Rutherford orbits. Refinements of the tunneling theory followed.^{15–17} The transfer of a nucleon between two nuclear surfaces depends upon the reduced widths of the nucleons in their bound states. However, Breit points out¹⁷ that theoretical problems make it difficult at present to obtain reliable values for reduced widths from transfer experiments. Such difficulties are compounded when the data sums over many final states in unknown proportions. It would appear that the appropriate nuclear parameters will be most readily extracted from single-nucleon transfer reactions proceeding between discrete initial and final states.

Single-nucleon transfer reaction experiments have dealt almost exclusively with the neutron as the transferring particle. The reason for this is the great simplicity of the aforementioned method for detecting the transfer by the decay of N^{13} . Transfer reactions in which a proton is the transferring nucleon should also be quite interesting. This paper presents differential cross section measurements for the two cases of proton transfer in the $N^{14}+B^{10}$ system, specifically from the target to the projectile and from the projectile to the target. For both reactions the experimental method insures that the residual nuclei are in their ground states. Boron-10 was selected as a target, since the ground-state transfer Q values are relatively small, thus making the assumption of Rutherford orbits more nearly valid. The reaction $B^{11}(N^{14},C^{13})C^{12}$ was also investigated to determine the possible effect of the high

positive Q value on the angular distribution. It is hoped that from experiments of this nature some insight as to the role of the Coulomb barrier on the transferred proton may also be gained.

II. EXPERIMENTAL

(a) Apparatus and Procedure

The experimental apparatus and procedure for collecting data was basically the two-detector coincidence system of Halbert and Zucker.¹⁸ In brief their system is as follows: one detector, the defining counter, is placed at the desired angle. A second detector, the conjugate counter, is then set at the correct angle to detect the recoiling reaction product. A coincidence is required before pulses from the defining counter are analyzed. The replacement of the original scintillation counters by surface-barrier detectors¹⁹ made it possible to study reactions in which good energy resolution is required. The kinematical criteria used in gating the multichannel analyzer to pulses from the defining counter, combined with the knowledge of the energy of the observed particle, are usually sufficient to identify a reaction unambiguously.

For the present investigation, however, the small positive Q value and the large elastic scattering counting rates from the target impurities resulted in possible confusion in certain angular ranges. A method of increasing the selectivity of the detection system and thus further eliminating spurious counts was devised. In a proton transfer reaction, the outgoing particle is of different charge than the elastically scattered particles. A measurement of the specific ionization, dE/dx , which depends upon the particle charge, makes it possible to eliminate virtually all the counts due to elastic scattering. To incorporate the added selectivity into the existing system, the defining counter was replaced by a proportional counter and surface-barrier detector combination.

Figure 1 illustrates the present defining counter. The particles enter the proportional counter through a 0.62-mg/cm² Ni entrance foil. The silicon surface-barrier counter, 800 ohm-cm n -type silicon, is located in the proportional counter atmosphere. No detrimental effects on the performance of either counter were noted. The length of the 1-mil diameter stainless steel wire is 2.3 cm. The counter was filled with a mixture of argon and 3% CO₂ to a pressure of about 5 cm Hg. Gas was flowed continuously at a rate of ≈ 2 cm³/min, and the pressure was held constant with a Manostat.²⁰ The proportional counter was operated at 400 v, and the silicon counter at 4 v. Nitrogen ions lose roughly 2 Mev in the entrance foil and 1 Mev in the gas before entering the silicon.

¹⁴ G. Breit and M. E. Ebel, Phys. Rev. **103**, 679 (1956).

¹⁵ G. Breit and M. E. Ebel, Phys. Rev. **104**, 1030 (1956).

¹⁶ G. Breit, *Handbuch der Physik* (Springer-Verlag, Berlin, 1959), Vol. 41, Part 1, pp. 367–407.

¹⁷ G. Breit, *Proceedings of the Second Conference on Reactions Between Complex Nuclei, Gatlinburg* (John Wiley & Sons, New York, 1960), pp. 1–15.

¹⁸ M. L. Halbert and A. Zucker, Phys. Rev. **115**, 1635 (1959).

¹⁹ M. L. Halbert and A. Zucker, Phys. Rev. **121**, 236 (1961).

²⁰ Model No. 8, Manostat Corporation, New York, New York.

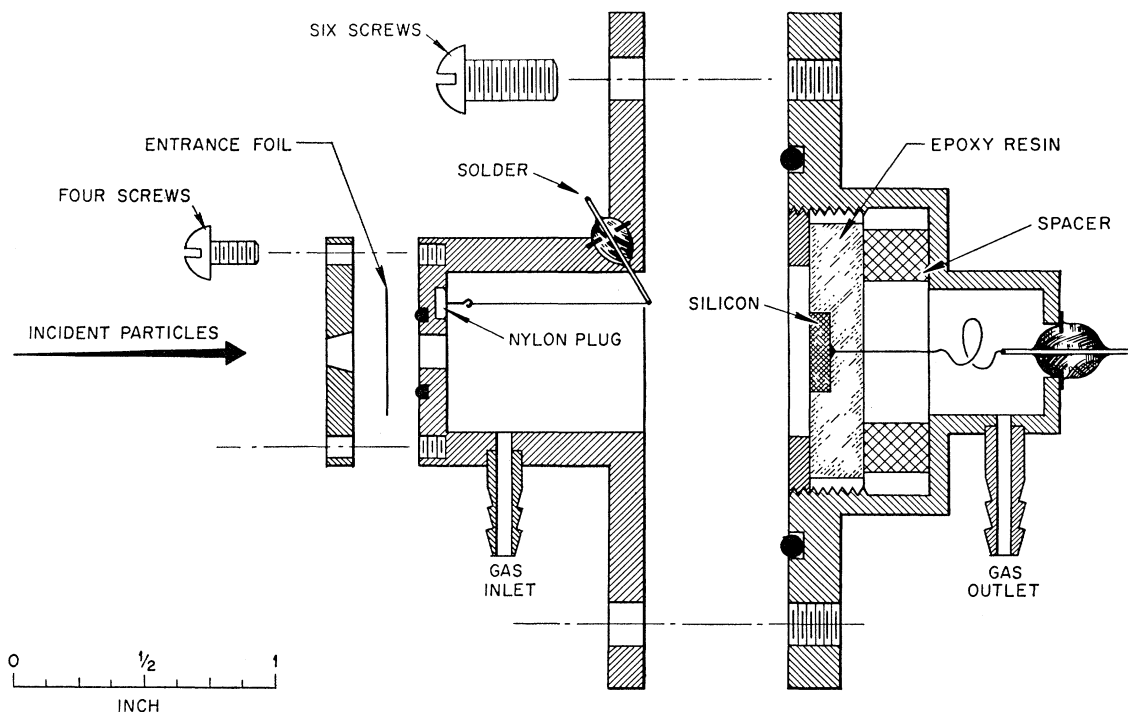


FIG. 1. The defining counter. The scattered particles enter the proportional counter through a 0.62-mg/cm^2 Ni entrance foil. After traversing the counter gas, the particles stop in an 800-ohm-cm n -type silicon-barrier counter. The surface-barrier counter is exposed to the proportional counter gas atmosphere. A mixture of argon and CO_2 flows continually through the counter.

The result of displaying dE/dx vs E on an oscilloscope²¹ is the separation of particles according to their charge. Figure 2 shows the dE/dx vs E spectrum for a B^{10} target at 30° in the laboratory. Proton and deuteron traces are absent in this photograph because their dE/dx pulses are indistinguishable from amplifier noise. The alpha line reaches a cutoff value and turns back due to insufficient barrier depth. The groups on the

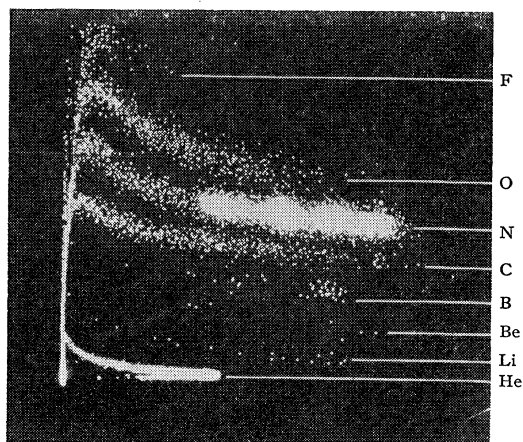


FIG. 2. A typical dE/dx vs E picture from the defining counter at 30° lab. The bright spots on the nitrogen charge line are elastically scattered particles from B^{10} , O, Si, and Fe. The latter three are target impurities.

²¹ C. D. Goodman and J. L. Need, Phys. Rev. **110**, 676 (1958).

nitrogen line in addition to the boron peak are due to scattering from target impurities. Starting at low energy, the peaks represent elastic scattering from B, O, Si, and Fe, respectively. Although the counter resolution is sufficient to separate different effective charges clearly, at these energies the difference in energy loss between isotopes is too small to permit isotopic identification.

To select the desired particles, the following procedure was used. Referring to the block diagram of the electronics, Fig. 3, the window of a single-channel analyzer was positioned on the dE/dx spectrum. The output of this analyzer was used to trigger the intensifying pulse for the dE/dx vs E oscilloscope trace and also as one input to a fast coincidence circuit. The window was first opened wide to obtain an oscilloscope display like that of Fig. 2. The window was then narrowed so that only the pertinent (i.e., high energy) portion of the desired charge line was displayed. The other input to the fast coincidence circuit was derived from the single-channel analyzer in the conjugate counter circuit. The position of this window was determined in the same manner as described in reference 14 with the exception that scattering from boron rather than carbon was used in the calibration. The output of the coincidence circuit was used to gate the 256-channel analyzer so as to record pulses from the defining counter.

Figure 4 shows the effect of the various coincidence gates for the $\text{B}^{10}(\text{N}^{14}, \text{O}^{15})\text{Be}^9$ reaction at 12° in the lab.

At the top is the ungated spectrum in the defining counter. The pulse height spectrum of the elastically scattered N^{14} particles is peaked in channel 120, and the O^{15} spectrum from the reaction is expected to peak in channel 99. The center spectrum illustrates the effect of gating with the recoil counter only. The recoil counter was positioned so as to detect the Be^9 . The elastic peak has been reduced substantially and the transfer peak may be seen to the left. There are two reasons for the persistence of the elastic peak. The first is that the energy of the Be^9 nuclei is very low at this angle, thus necessitating the lowering of the window on the conjugate counter. This increases the random rate due to the fact that recoiling B^{10} nuclei from elastic scattering (at a very small center-of-mass angle and, therefore, large cross section) now also appear in the window. The second is that multiple scattering of the low energy elastic recoils in the target causes them to appear at the "incorrect" recoil angle, thereby producing real coincidences with the elastic N^{14} . The lowest spectrum in Fig. 4 illustrates the combined effect of charge state selection plus kinematical criteria. The background has been reduced to essentially zero and the peak corresponding to the ground state transfer stands clearly defined.

B. Targets

Thin targets of enriched B^{10} and B^{11} were prepared in the following manner.²² The enriched source material was packed tightly into a high-purity carbon tube machined from a $\frac{1}{4}$ -in. diameter spectroscopic electrode. A typical charge weighed about 300 mg. The carbon completely enclosed the powder except for a $\frac{1}{16}$ -in. slot milled lengthwise into the cavity. The cylinder was heated slowly in a vacuum evaporator, so that the evaporation could take place at as low a pressure as possible. At a current of approximately 280 amp, which

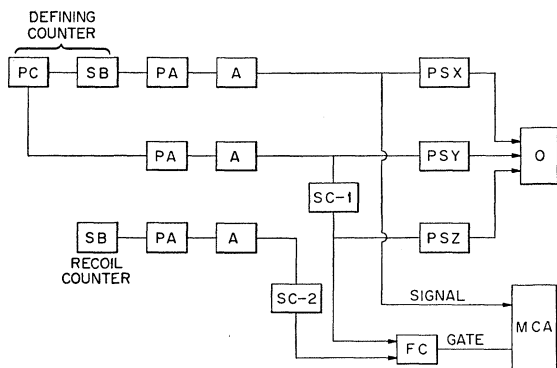


FIG. 3. Block diagram of the electronics. The legend is as follows: S.B.—silicon barrier detector, P.C.—proportional counter, P.A.—pre-amplifier, A.—amplifier, S.C.—single-channel analyzer, P.S.—pulse stretcher, F.C.—fast coincidence, O.—oscilloscope, M.C.A.—256-channel analyzer.

²² G. R. Hoke and E. Newman, Oak Ridge National Laboratory Report ORNL-3021 (unpublished).

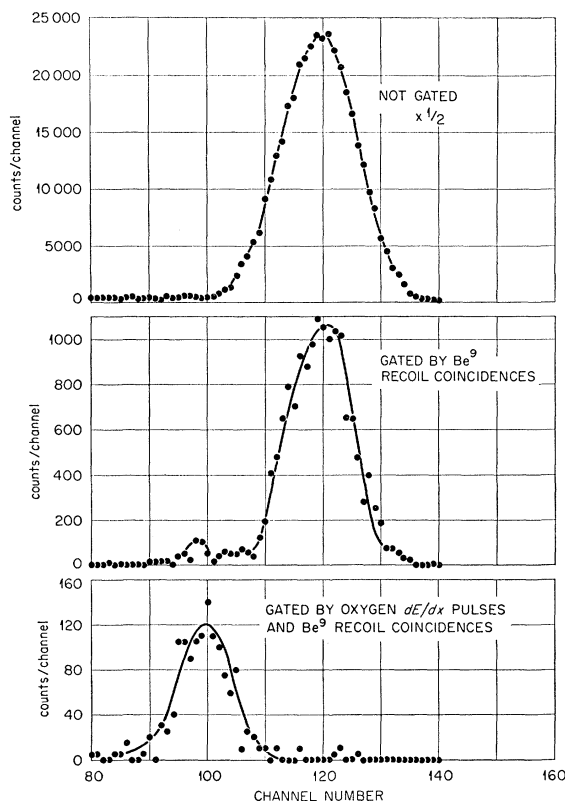


FIG. 4. Coincidence-gated spectra of the defining surface-barrier counter at 12° lab. Reading from top to bottom the spectra represent an ungated run, gated by recoils only, and gated by recoils-plus-charge selection. The peak due to the ground-state transfer $B^{10}(N^{14}, O^{15})Be^9$ is seen to the left of the elastic peak in the spectrum gated by Be^9 recoil coincidences.

corresponded to a temperature greater than $2400^\circ C$, the boron vaporized and was collected on glass plates. The resultant film was then floated off the glass in a tray of water and picked up on a target frame. These films were self-supporting and averaged about $100 \mu g/cm^2$ thick. This thickness corresponds to an energy loss for the beam of about 600 kev. During the experiment several impurities were noted in the target, namely: carbon, oxygen, silicon, and iron.

III. RESULTS

$B^{10}(N^{14}, O^{15})Be^9$ ground states. The differential cross section of the reaction in which a proton is transferred from a B^{10} target nucleus to the incident N^{14} ion is presented in the upper curve of Fig. 5. The reaction products, O^{15} and Be^9 , are both in their ground states. The mean energy of the N^{14} beam at the center of the target was 27.5 Mev and the Q of the reaction is $+0.704$ Mev.²³ The points designated by circles are data taken with the recoil coincidence technique only, and the squares with the recoil-plus-charge identification

²³ F. Everling, L. A. Konig, J. H. E. Mattauch, and A. H. Wapstra, Nuclear Phys. 18, 529 (1960).

method. Open points are upper limits on the cross section. The cross section rises to a peak value of 1.3 mb/sr at $\approx 30^\circ$ in the center-of-mass system. The bars on the experimental points are standard deviations and include random errors. The accuracy of the absolute scale is difficult to evaluate. The targets were weighed after bombardment, but subtraction of the weights of the target impurities made the B^{10} target thickness the largest single source of uncertainty. An over-all evaluation of the possible systematic errors indicates that a $\pm 20\%$ error in the absolute scale is reasonable.

The total cross section for the ground-state transfer is 1.34 ± 0.30 mb. The total cross section to all states for the $B^{10}(N^{14}, O^{15})Be^9$ reaction may be estimated to be ≈ 5 mb. This estimate is based on the fact that when the cross section for neutron transfers is plotted as a function of E^* , where:

$$E^* = E_{c.m.} - E_{barr} + Q,$$

a "universal" curve is obtained.⁵ Although there is insufficient evidence for the existence of a similar universal curve for proton transfers, approximately the same total cross section was inferred in reference 4 from experimental measurements on this reaction. Thus, transfers leaving the residual nuclei in excited states contribute significantly to the cross section.

$B^{10}(N^{14}, C^{13})C^{11}$ ground states. In this reaction the incident N^{14} ion loses a proton to the B^{10} target nucleus. The Q value is $+1.142$ Mev.²³ The lower portion of Fig. 5 is a plot of the differential cross section as a function of the center-of-mass angle Θ . The cross section reaches its peak value of 2.78 mb/sr at an angle of $\approx 28^\circ$. All experimental points on this curve were taken with the recoil-plus-charge identification technique. The measurements were terminated at 40° in the center-of-mass system because of low counting rates.

The integrated ground-state cross section for this

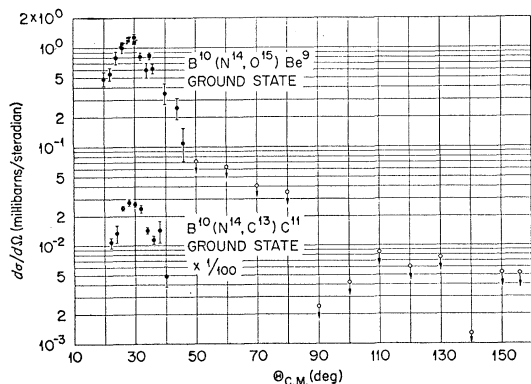


FIG. 5. Upper curve—differential cross section for the transfer reaction $B^{10}(N^{14}, O^{15})Be^9$ ground state. Points designated by circles were taken by the recoil coincidence technique only, squares with recoil-plus-charge identification. Open points are upper limits of the cross section. Lower curve—differential cross section for the transfer reaction $B^{10}(N^{14}, C^{13})C^{11}$ ground state. All data were taken with the recoil-plus-charge identification technique.

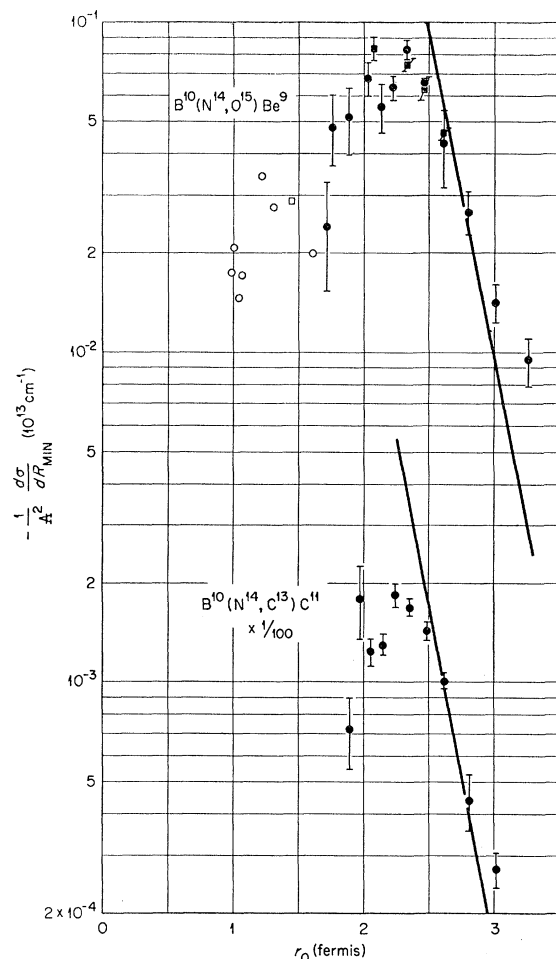


FIG. 6. Top—the differential cross section $d\sigma/dR_{min}$ plotted against r_0 for the reaction $B^{10}(N^{14}, O^{15})Be^9$. The significance of the types of points are the same as Fig. 5. Bottom—the differential cross section $d\sigma/dR_{min}$ plotted against r_0 for the reaction $B^{10}(N^{14}, C^{13})C^{11}$. The curves are calculated from the tunneling theory of Breit¹⁷ as given in Eq. (5) and are normalized to the data.

reaction is 2.19 ± 0.49 mb. The cross section for all states has been measured to be ≈ 4.5 mb at 27-Mev incident ion energy.⁴ As for the previous case, it is seen that excited state transfers must contribute appreciably to the total cross section.

$B^{11}(N^{14}, C^{13})C^{12}$ ground states. The effect of the Q value on the ground-state cross section and on the angular distribution should show up in this reaction, since Q is very large, namely, $+8.407$ Mev.²³ Because of this high Q a large portion of the angular range could be investigated without any coincidence requirements. For angles smaller than 20° in the center-of-mass system, an absorber was placed in front of the detector to stop the elastically scattered N^{14} (≈ 27 Mev) but to allow the more energetic C^{13} (≈ 35 Mev) to be detected. In this way the investigation was carried to 4° (c.m.).

No counts were detected in the correct portion of the spectrum which could be unambiguously assigned to

the reaction. An upper limit for the cross section is placed at $25 \mu\text{b/sr}$ in the angular region from 4° to 60° (c.m.). Integrating this value from 0° to 180° , the total cross section is $<300 \mu\text{b}$.

IV. DISCUSSION

The tunneling theory treats the initial and final particles by assuming they are traveling on classical Rutherford orbits. The motion of the nucleon which is tunneling between the two nuclear surfaces is treated quantum mechanically.

A method of plotting the angular distribution data which facilitates the comparison of theory and experiment has been initiated by McIntyre.¹¹ The quantity $d\sigma/dR_{\min}$ is plotted as a function of R_{\min} , where R_{\min} is the distance of closest approach along a Rutherford orbit giving the same angular deflection as that for the observed particle. The relationship between $d\sigma/d\Omega$ and $d\sigma/dR_{\min}$ is:

$$d\sigma/dR_{\min} = -(8\pi/a) \sin^3(\Theta/2) (d\sigma/d\Omega), \quad (1)$$

where

$$a = Z_1 Z_2 e^2 / 2E_{\text{c.m.}}, \quad (2)$$

and

$$R_{\min} = a[1 + \csc(\Theta/2)]. \quad (3)$$

Breit¹⁷ has suggested that the theory in its present form is more directly related to a plot of $\ln(\lambda^2 d\sigma/dR_{\min})$ against R_{\min} , where λ is the center-of-mass wavelength divided by 2π . The upper and lower portions of Fig. 6 show, respectively, the $\text{B}^{10}(\text{N}^{14}, \text{O}^{15})\text{Be}^9$ and $\text{B}^{10}(\text{N}^{14}, \text{C}^{13})\text{C}^{11}$ results plotted in this manner where r_0 has been substituted for R_{\min} . The parameter r_0 is related to R_{\min} by

$$R_{\min} = r_0(A_1^{1/3} + A_2^{1/3}). \quad (4)$$

It is seen that both reactions peak at a value of $r_0 = 2.15 \pm 0.1$ fermis. This value is the same as the $r_0 \approx 2.2$ fermis obtained⁹ for ground-state neutron transfers.

It was of some interest to determine how well the tunneling theory would reproduce the experimental

results despite the fact that no attempt has been made to include any possible effect of the Coulomb field on the transferring proton. The relationship between $d\sigma/dR_{\min}$ and R_{\min} is given by¹⁷

$$d\sigma/dR_{\min} \propto \lambda^2 \exp[-\alpha R_{\min} - \bar{\alpha} \bar{R}_{\min}], \quad (5)$$

where

$$\alpha = [(2M/\hbar^2)E_s]^{1/2}; \quad \bar{\alpha} = [(2M/\hbar^2)\bar{E}_s]^{1/2}, \quad (6)$$

and E_s and \bar{E}_s are the separation energies of the transferring nucleon of mass M in the delivering and accepting nuclei, respectively. The predictions of Eq. (5) normalized to the experimental data are also shown in Fig. 6. The fit is indeed good; it reproduces the initial slope quite accurately. This is to be compared with the rather poor fit to the ground-state neutron transfers of reference 9.

In conclusion then it would appear that the cross section for transfers leaving one or both reaction products in an excited state is appreciable for proton as well as neutron transfer reactions. The very small cross section in the $\text{B}^{11}(\text{N}^{14}, \text{C}^{13})\text{C}^{12}$ ground-state reaction is puzzling. It may be that the reduced widths for this transition is abnormally small, but perhaps a more realistic possibility is that high- Q transfers populate excited states preferentially. In comparing the shapes of the ground-state proton and neutron⁹ transfer angular distributions, it may be noted that the former are narrower. It is possible that this difference may be caused by the effect of the Coulomb field on the transferring proton.

ACKNOWLEDGMENTS

The author wishes to thank A. Zucker for suggesting this problem, for his help and encouragement during the performance of the experiment, and for the design of the proportional counter. Appreciation is expressed to K. S. Toth and M. L. Halbert for many interesting and helpful discussions, G. A. Palmer for assistance in taking data, A. W. Riikola and H. L. Dickerson for the operation of the cyclotron, and J. G. Harris for construction of the apparatus.

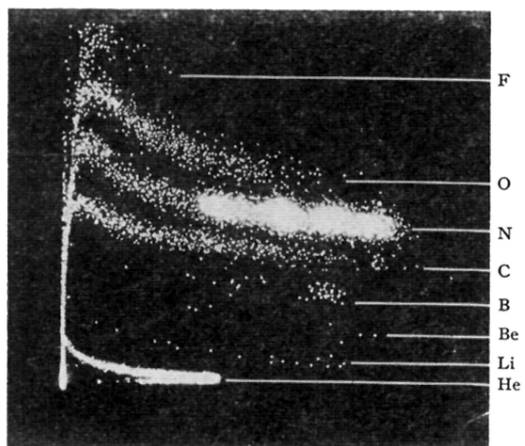


FIG. 2. A typical dE/dx vs E picture from the defining counter at 30° lab. The bright spots on the nitrogen charge line are elastically scattered particles from B^{10} , O, Si, and Fe. The latter three are target impurities.